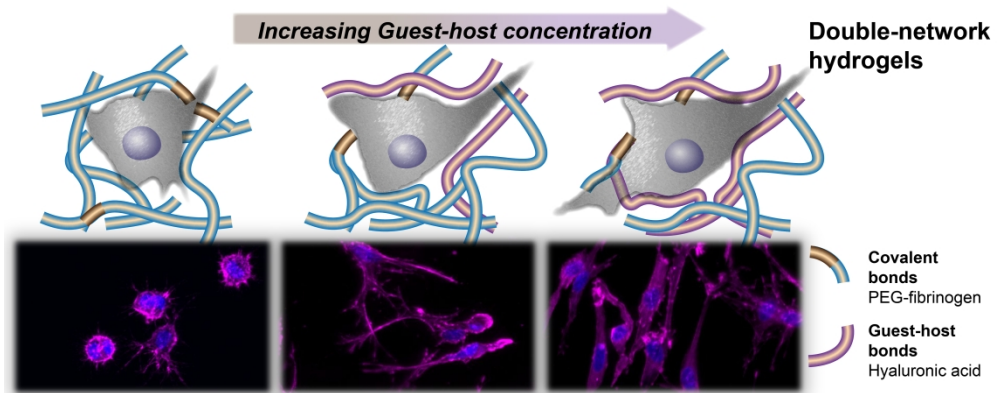


**Tailoring supramolecular guest-host hydrogel viscoelasticity  
with covalent fibrinogen double networks**

Journal:	<i>Journal of Materials Chemistry B</i>
Manuscript ID	TB-ART-10-2018-002593.R1
Article Type:	Paper
Date Submitted by the Author:	20-Nov-2018
Complete List of Authors:	Loebel, Claudia; University of Pennsylvania, Bioengineering Ayoub, Amal; Technion Israel Institute of Technology, Biomedical Engineering Galarraga, Jonathan; University of Pennsylvania, Bioengineering Kossover, Olga; Technion Israel Institute of Technology, Biomedical Engineering Simaan-Yameen, Haneen; Technion Israel Institute of Technology Seliktar, Dror ; Technion Israel Institute of Technology, Biomedical Engineering Burdick, Jason; University of Pennsylvania, Bioengineering



1 **Tailoring supramolecular guest-host hydrogel viscoelasticity with covalent fibrinogen**  
2 **double networks**

3

4 *Claudia Loebel<sup>1</sup>, Amal Ayoub<sup>2</sup>, Jonathan H. Galarraga<sup>1</sup>, Olga Kossover<sup>2</sup>, Haneen Simaan-*  
5 *Yameen<sup>2</sup>, Dror Seliktar<sup>2</sup>, Jason A. Burdick<sup>1\*</sup>*

6

7 <sup>1</sup>Department of Bioengineering, University of Pennsylvania, 210 South 33rd Street,  
8 Philadelphia, PA 19104, USA

9 <sup>2</sup>Institute of Technology, Faculty of Biomedical Engineering, Technion-Israel Institute of  
10 Technology, Technion City, Haifa 32000, Israel

11

12 \*Corresponding author: burdick2@seas.upenn.edu, phone: +1-215-898-8537, fax: +1-215-573-  
13 2071

14

15 **Keywords**

16 Hydrogels, double networks, viscoelasticity, hyaluronic acid, MSCs

17

18 **Abstract**

19 Supramolecular chemistry has enabled the design of tunable biomaterials that mimic the  
20 dynamic and viscoelastic characteristics of the extracellular matrix. However, the noncovalent  
21 nature of supramolecular bonds renders them inherently weak, limiting their applicability to  
22 many biomedical applications. To address this, we formulated double network (DN) hydrogels  
23 through a combination of supramolecular and covalent networks to tailor hydrogel viscoelastic  
24 properties. Specifically, DN hydrogels were formed through the combination of supramolecular  
25 guest-host (GH) hyaluronic acid (HA) networks with covalent networks from the  
26 photocrosslinking of acrylated poly(ethylene glycol) modified fibrinogen (PEG-fibrinogen) and  
27 PEG diacrylate. DN hydrogels exhibited higher compressive moduli, increased failure stresses,  
28 and increased toughness when compared to purely covalent networks. While GH concentration  
29 had little influence on the compressive moduli across DN hydrogels, an increase in the GH  
30 concentration resulted in more viscous behavior of DN hydrogels. High viability of encapsulated  
31 bovine mesenchymal stromal cells (MSCs) was observed across groups with enhanced  
32 spreading and proliferation in DN hydrogels with increased GH concentration. This combination  
33 of supramolecular and covalent chemistries enables the formation of dynamic hydrogels with  
34 tunable properties that can be customized towards repair of viscoelastic tissues.

## 35 Introduction

36 Synthetic hydrogels offer a versatile spectrum of mechanical and chemical properties to  
37 replicate aspects of native tissues or to systematically investigate their influence on biological  
38 processes<sup>1, 2</sup>. As such, hydrogels play central roles in approaches to the engineering of tissues,  
39 as well as three-dimensional (3D) culture systems to understand cell behavior<sup>3</sup>. However, many  
40 of the synthetic hydrogels used in these approaches exhibit static and elastic characteristics,  
41 which do not capture the dynamic complexity of native extracellular matrix (ECM). To address  
42 this, hydrogels have been engineered to change over time through network erosion processes,  
43 including those sensitive to proteolytic<sup>4-6</sup> or hydrolytic<sup>7, 8</sup> degradation. More recently, hydrogels  
44 are being designed to increase their viscoelastic behavior, including through control over stress-  
45 relaxation<sup>9-11</sup> or by introducing reversible crosslinking<sup>12, 13</sup>, to better emulate ECM dynamics.

46 Despite these advances in the design of viscoelastic hydrogels, there are limitations to  
47 such approaches, particularly as the use of non-covalent crosslinking can decrease the overall  
48 mechanical resilience and stability of hydrogels and limit their applications in the repair of  
49 viscoelastic tissues. To address this, hydrogels based on double network (DN) structures have  
50 evolved as promising materials for tissue repair strategies, owing to their high toughness and  
51 high water content<sup>14</sup>. DN hydrogels represent a subset of interpenetrating polymer networks  
52 (IPNs) and are defined by a primary network that is highly crosslinked and typically brittle, and a  
53 secondary ductile but weak network<sup>15</sup>. The asymmetric nature of these two entangled networks  
54 results in hydrogels with improved strength and toughness primarily through chain entanglement  
55 and energy dissipation mechanisms<sup>16</sup>. Indeed, the natural ECM consists of networks of  
56 numerous proteins and sugars, which contribute to the complex mechanical properties of  
57 tissues.

58 Critical for the design of these tough DN hydrogels is the ability of the secondary  
59 network to self-heal, which is often achieved by dynamic bond rupture and reforming upon  
60 deformation. In particular, physical networks, including those based on ionic<sup>17-19</sup>, hydrogen<sup>20</sup>,  
61 and supramolecular<sup>21, 22</sup> bonding have enabled the formation of DN hydrogels with self-healing  
62 network properties that protect the primary network from failure. While some of these systems  
63 have been optimized towards viable cell encapsulation<sup>17, 18, 23</sup>, the static and elastic nature of the  
64 primary network and the resulting DN may restrict cell functions such as morphological changes  
65 that are critical towards cell proliferation and new tissue formation.

66 Here, we developed a DN hydrogel system that incorporates high strength and  
67 toughness, while still maintaining encapsulated cell activity, and applied this system to elucidate  
68 the role of viscoelasticity on cell behavior. To accomplish this, the primary network comprised

69 fibrinogen modified with acrylated poly(ethylene)glycol (PEG) and optional PEG-diacrylate,  
70 which was photocrosslinked and conserved the bioactivity and degradability of the fibrinogen  
71 backbone<sup>24-26</sup>. For the secondary network, we employed supramolecular guest-host (GH)  
72 interactions to assemble the network with supramolecular bonds through the complex of  $\beta$ -  
73 cyclodextrin (CD, host) and adamantane (Ad, guest), which were separately coupled to  
74 hyaluronic acid (HA)<sup>27, 28</sup>.

75 The combination of covalent PEG-fibrinogen and supramolecular GH networks enabled  
76 the formation of DN hydrogels with independent control over the viscous and elastic properties,  
77 which holds promise for repairing native tissues and as 3D culture systems *in vitro*.

78

## 79 **Experimental**

### 80 ***Material synthesis and characterization***

81 All chemicals were purchased from MilliporeSigma unless otherwise indicated.

82 Hyaluronic acid (HA, 75 kDa; Lifecore Biomedical) was converted to the  
83 tetrabutylammonium salt (HA-TBA) by ion exchange against Dowex 50Wx8 hydrogen form and  
84 neutralized with aqueous tetrabutylammonium hydroxide (0.4 M)<sup>8</sup>. HA-TBA was modified with 1-  
85 adamantane acetic acid (Ad) to form Ad-HA (Fig. S1) or 6-(6-aminohexyl)amino-6-deoxy- $\beta$ -  
86 cyclodextrin (CD) to form CD-HA (Fig. S2) by anhydrous reaction in DMSO, according to our  
87 previously published methods<sup>27</sup>. Briefly, coupling of adamantane (3.0 equiv) to HA (1 equiv  
88 disaccharides) was performed by an esterification reaction with di-tert-butyl decarbonate  
89 ( $\text{Boc}_2\text{O}$ , 0.54 equiv) and 4-dimethylaminopyridine (DMAP, 1.5 equiv). Coupling of cyclodextrin  
90 (0.6 equiv) to HA (1 equiv) was performed by reaction in the presence of (benzotriazol-1-  
91 yloxy)tris(dimethylamino)phosphonium hexafluorophosphate (BOP, 0.6 equiv). For all HA  
92 derivatives, purification was performed by dialysis and lyophilization, and functionalization of the  
93 polymers was quantified by <sup>1</sup>H NMR (Bruker 360 MHz) as previously described<sup>27</sup>.

94 Synthesis of PEG-fibrinogen was performed from linear PEG as previously described  
95 (10 kDa)<sup>24</sup>. Briefly, PEG-diacrylate (PEG-DA, Fig. S3) was obtained by reacting PEG-OH (1  
96 equiv) under argon with acryloyl chloride (1.5 equiv) and triethylamine (1.5 equiv) in  
97 dichloromethane. Bovine fibrinogen (1 equiv) was covalently coupled to PEG-DA (145 equiv) in  
98 an 8 M urea solution in the presence of tris (2-carboxyethyl) phosphine hydrochloride (TCEP  
99 HCl, 68 equiv). The PEG-fibrinogen product was precipitated in acetone and dialyzed.

100

101

102

### 103 **Hydrogel formation**

104 Ad-HA and CD-HA of 29% and 25% modification, respectively, were used for all experiments  
105 and the GH concentration (0, 3, 5%) denotes the combined polymer weight percent, while  
106 maintaining a 1:1 ratio of adamantane and  $\beta$ -cyclodextrin. DN hydrogels were prepared from  
107 separate solutions of Ad-HA and CD-HA dissolved in PEG-fibrinogen to obtain a final  
108 concentration of 8.5 mg/mL PEG-fibrinogen in PBS containing 0.05% 2-hydroxy-4'-(2-  
109 hydroxyethoxy)-2-methylpropiophenone (Irgacure 2959) photoinitiator. The concentration of  
110 PEG-DA (1, 2, 3%) indicates the weight percent of additional PEG-DA added. The two-  
111 component solution was manually mixed and briefly centrifuged to remove entrapped air.  
112 Hydrogels were cast into ca. 300  $\mu$ m thick films between two coverslips and photocrosslinked  
113 with ultraviolet (UV) light (EXFO OmniCure Series 1500, 320-390 nm filter, 5 mW cm<sup>-2</sup>, 5 min).

### 115 **Mechanical characterization**

116 Shear rheology: Hydrogels were formed as described and rheological properties were examined  
117 using an AR2000 stress-controlled rheometer (TA Instruments) fitted with a 20 mm diameter  
118 cone and plate geometry and 27  $\mu$ m gap. Rheological properties were measured by oscillatory  
119 frequency sweeps (0.01-100 Hz; 1% strain), oscillatory time sweeps (0.1 Hz, 1% strain) and  
120 oscillatory strain sweeps (0.01-500% strain).

121 Dynamic mechanical analysis: Compressive moduli were examined by dynamic  
122 mechanical analysis (TA Instruments, Q800, 0.5 N min<sup>-1</sup>). Hydrogels were cast into 5 mm  
123 diameter cylinders, secured via a preload (0.01 N), and compressed (0.5 N min<sup>-1</sup>) to determine  
124 the Young's moduli (slope from 10-20% strain), failure strains and failure stresses.

125 Tensile testing: Hydrogels were cast into dog-bone shaped samples using  
126 polydimethylsiloxane (PDMS) molds (3.0 mm thick, 5.0 width at center). Samples were secured  
127 using custom clamps with pre-tension (0.01 N) and then extended at 5.0 mm sec<sup>-1</sup> (Instron  
128 5848, 5 N load cell). Engineering stress-strain curves were employed to measure tensile moduli  
129 (slope from 40-50% strain), failure strains and failure stresses. Toughness was determined by  
130 integration of the area under stress-strain profiles.

### 132 **Cell encapsulation, viability and immunofluorescence**

133 Bovine mesenchymal stromal cells (MSCs) were isolated from bone marrow of calves (4-6  
134 months old) obtained from Research 87 Inc (Boylston, MA, USA), as previously described<sup>29</sup>.  
135 MSCs were passaged once in high glucose Dulbecco's modified Eagle's Medium (DMEM, 10%

136 fetal bovine serum, 1% penicillin streptomycin) and encapsulated at a density of  $5 \times 10^6$  cells mL<sup>-1</sup>. Hydrogels were prepared as described and cultured for one day (24 hours) or three days.

138 Viability was assessed by fluorescent staining with calcein AM (2  $\mu$ M) and ethidium  
139 homodimer-1 (4  $\mu$ M) for 30 min, imaging with an Olympus epifluorescent microscope, and  
140 quantifying with ImageJ software.

141 For immunofluorescence staining, hydrogels were fixed with 10% buffered formaldehyde  
142 in PBS at RT for 30 min, permeabilized with 1% Triton X100 (2 hours, 4 °C) and stained with  
143 rhodamine-conjugated phalloidin (1:100 in 1% bovine serum albumin; Invitrogen R415) for 2  
144 hours at RT, followed by incubation in 5  $\mu$ g/mL Hoechst 33342 for 30 min. Z-stack images were  
145 acquired on a Nikon A1R Confocal Microscope at 20x0.75 NA and 40x0.95 NA.

146 MSC proliferation was assessed using 5-ethynyl-2'-deoxyuridine (EdU) incorporation  
147 over three days in culture. Upon fixing as described, EdU was visualized with AlexaFlour 488  
148 azide using the Click-iT EdU kit according to the manufacturer's instructions (Thermofisher  
149 Scientific). Cell nuclei were counterstained with Hoechst before confocal imaging and the  
150 fraction of proliferating cells was quantified as the fraction of nuclei stained positive for EdU.

151

## 152 **Statistical analysis**

153 All experiments were performed with three replicates, and statistical significance was assessed  
154 using GraphPad Prism 7 software. Comparisons among groups were made using one-way  
155 ANOVA with Bonferroni *post hoc* testing.

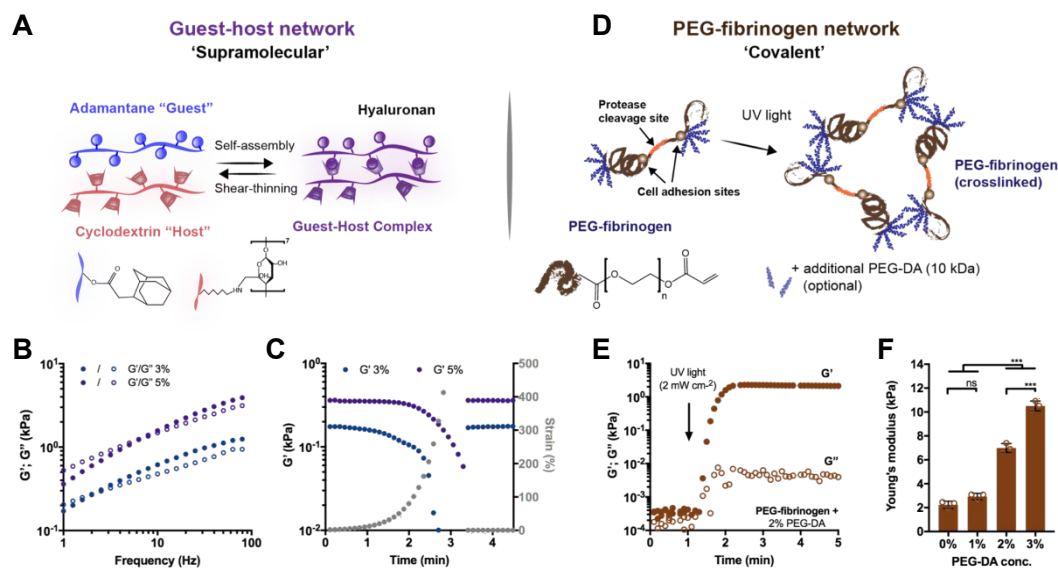
156

## 157 **Results & discussion**

### 158 **Single networks have tunable properties**

159 The supramolecular network is based on reversible GH complexes between Ad and CD  
160 moieties coupled to HA and a GH hydrogel is formed immediately upon mixing of the separate  
161 Ad-HA and CD-HA polymer solutions (Fig. 1A). Oscillatory shear rheology confirmed the  
162 expected frequency dependence of the storage and loss moduli ( $G'$  and  $G''$ , Fig. 1B), due to the  
163 dynamic bonding of Ad and CD. As expected, the GH hydrogel moduli increased with  
164 increasing concentration of GH polymers. To examine the response of the GH network to  
165 increased strains and subsequent recovery, such as upon deformation or loading, hydrogels  
166 were subjected to increasing oscillatory strains (0.05 - 500%) followed by low strain (1%). Strain  
167 sweeps indicated a decrease in moduli with increasing strains, with yielding at high strains  
168 (~90% strain at yield) (Fig. 1C). The network exhibited a rapid recovery to the initial modulus  
169 ( $G' = 0.37 \pm 0.14$  kPa, 5% GH) within seconds of the transition back to low strain (Fig. 1C).

170 Again, network properties were altered through the concentration of GH polymer, where lower  
 171 concentrations resulted in an overall reduction in modulus ( $G' = 0.23 \pm 0.21$  kPa, 3% GH), but  
 172 still exhibited yielding and self-healing behaviors (Fig. 1C). Thus, such a GH system exhibits  
 173 the desired self-healing and tunable properties of a dynamic network.



174  
 175 **Figure 1 Double network (DN) hydrogels consist of two independent polymer networks with**  
 176 **controlled properties.**

177 **A** Schematic illustrating adamantane (Ad-HA, blue) and  $\beta$ -cyclodextrin (CD-HA, red) modified hyaluronic  
 178 acid (HA) supramolecular assembly through guest-host (GH, purple) bond formation. Representative **B**  
 179 frequency sweeps (1.0-100 Hz, 0.5% strain) and **C** strain sweeps (1.0 Hz, 1-500% strain, then recovery to  
 180 1% strain) of storage ( $G'$ , filled symbols) and loss ( $G''$ , empty symbols) moduli of GH hydrogels at  
 181 concentrations of 3% (blue) and 5% (purple). **D** Schematic illustrating PEG-fibrinogen that contains  
 182 natural protease cleavage and cell adhesion sites and is functionalized with acrylated poly(ethylene  
 183 glycol) (PEG), through reaction with PEG-diacrylate (PEG-DA). To form hydrogels, unreacted acrylate  
 184 groups on PEG-fibrinogen and optional additional PEG-DA are polymerized with ultraviolet light in the  
 185 presence of a photoinitiator (I2959). **E** Representative time sweep (1.0 Hz, 0.5% strain) of the crosslinking  
 186 of PEG-fibrinogen hydrogels (8.5 mg/ml) with 2% PEG-DA. **F** Young's moduli of PEG-fibrinogen (8.5  
 187 mg/ml) with varying concentrations of PEG-DA (mean  $\pm$  SD, \*\*\* $p \leq 0.001$ , ns = no significant difference by  
 188 one-way ANOVA with Bonferroni *post hoc*).  
 189

190 The covalent network is comprised of a fibrinogen backbone with reactive end groups  
 191 (acrylated PEG-fibrinogen) and PEG-DA, and is formed through a photocrosslinking mechanism  
 192 (Fig. 1D). Photopolymerization, in the presence of UV light and a radical generating  
 193 photoinitiator (Irgacure 2959), resulted in the formation of PEG-fibrinogen hydrogels, which  
 194 exhibited primarily elastic properties ( $\tan \delta < 0.01$ ) due to the covalent crosslinking  
 195 (Fig. 1E). The elasticity of the network was altered by adjusting the PEG-DA content, resulting in  
 196 variable moduli (Young's modulus:  $2.23 \pm 0.35$  to  $10.51 \pm 0.41$  kPa), which was independent of  
 197 the fibrinogen concentration (constant at 8.5 mg/mL, Fig. 1F). The results confirm that the single



198 network hydrogels have distinct properties from each other, based on their respective mode of  
199 crosslinking (i.e., supramolecular versus covalent bonds).

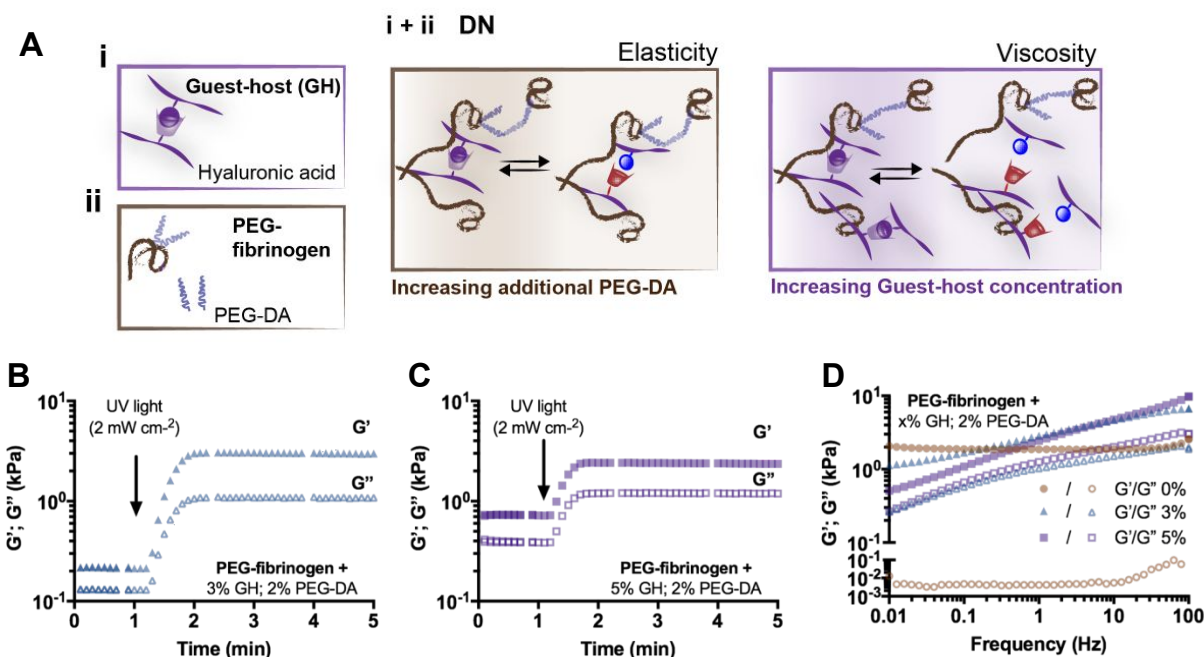
200

### 201 ***DN hydrogels exhibit viscoelastic properties***

202 Given the precise control over the properties of either network, we expected that the  
203 combination of supramolecular and covalent networks would enable facile tuning of the elasticity  
204 and viscosity of DN hydrogels (Fig. 2A). When GH and PEG-fibrinogen/PEG-DA polymers were  
205 mixed in solution, hydrogels were initially soft due to the rapid self-healing of the GH bonds, but  
206 the elastic and viscous moduli then increased when exposed to UV light due to covalent PEG-  
207 DA (2%) crosslinking ( $G'$ :  $2.48 \pm 0.13$  kPa,  $G''$ :  $0.82 \pm 0.12$  kPa, Fig. 2B). GH bonds contributed  
208 largely to the properties of the DN hydrogels, as network entanglement and supramolecular  
209 bond formation resulted in a viscous modulus two orders of magnitude greater than that of the  
210 covalent only crosslinked PEG-fibrinogen/PEG-DA alone (0% GH, Fig. 1E). Next, the GH  
211 polymer concentration was increased to 5% while maintaining the PEG-DA concentration at 2%  
212 (Fig. 2C). Although this resulted in a minimal change in the elasticity ( $G'$ :  $2.59 \pm 0.38$  kPa), the  
213 viscous modulus increased similarly to the trend observed within single GH networks ( $G''$ :  $1.34$   
214  $\pm 0.23$  kPa).

215 The frequency response of the hydrogels was investigated and further illustrated the  
216 variability in network structure for the DN hydrogels based on the composition (Fig. 2D).  
217 Specifically, while 0% GH hydrogels resulted in steady elastic and viscous moduli across the  
218 frequency range ( $G'$ :  $2.14 \pm 0.16$  kPa,  $G''$ :  $0.005 \pm 0.001$  kPa), DN hydrogels exhibited  
219 frequency dependent moduli, as indicated by reductions of  $G'$  and  $G''$  at low frequencies (Fig.  
220 2D). In both 3% and 5% DN hydrogels, material properties were dominated by the elastic moduli, which  
221 was attributed to the covalent network structures. These results suggest that supramolecular  
222 bonds are conserved within DN hydrogels, enabling viscoelastic behavior dependent on the polymer  
223 concentration of the GH network.

224



225

### 226 **Figure 2 DN hydrogels exhibit viscoelastic properties.**

227 **A** Schematic illustrating DN network formation through the combination of (i) guest-host (GH) network and  
 228 (ii) covalently crosslinked PEG-fibrinogen (8.5 mg/mL) with or without additional PEG-DA. Schematics of  
 229 network tunability where viscoelasticity of DN hydrogels is controlled through the amount of additional  
 230 PEG-DA (elasticity) and the GH concentration (viscosity). Representative time sweeps (1.0 Hz, 0.5%  
 231 strain) of storage ( $G'$ , filled symbols) and loss ( $G''$ , empty symbols) moduli of DN hydrogels (PEG-  
 232 fibrinogen (8.5 mg/mL) plus 2% PEG-DA) containing either **B** 3% or **C** 5% GH concentration. **D**  
 233 Representative frequency sweeps (0.01-100 Hz, 0.5% strain) of DN hydrogels (PEG-fibrinogen (8.5  
 234 mg/mL) plus 2% PEG-DA) without (0%) or with (3% or 5%) GH of different concentrations.

235

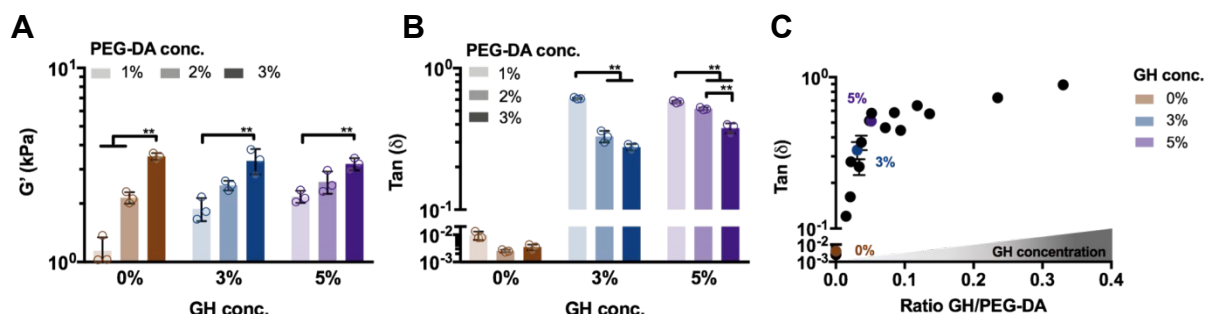
236

### 237 **Viscous and elastic properties of DN hydrogels are tuned independently**

238 Noting that DN hydrogels displayed dynamic properties, the influence of the DN composition on  
 239 the viscoelasticity of the system was investigated. These inputs (e.g., polymer concentration,  
 240 ratio of supramolecular to covalent crosslinking) govern the configurations in which the networks  
 241 may assemble and could influence DN crosslink densities, structural inhomogeneities and  
 242 entanglements, which may impact energy dissipation mechanisms<sup>30</sup>. Therefore, the  
 243 concentration of individual polymers, either GH or PEG-DA, was altered and DN hydrogel  
 244 properties were systematically investigated by rheology.

245 To evaluate how hydrogel composition influenced elastic properties, storage moduli of  
 246 various DN compositions were examined. PEG-DA concentration was found to exhibit a greater  
 247 influence over the elastic modulus than the GH concentration across formulations (Fig. 3A). For  
 248 instance, an increase in PEG-DA concentration from 1 to 3% resulted in a 47-77% increase in

249 the elastic modulus, whereas an increase in the GH concentration from 0 to 3% resulted in  
 250 negligible changes. While these findings demonstrate the impact on DN hydrogel elasticity, the  
 251 utilization of DNs to control viscous behavior has rarely been investigated<sup>18</sup>. To evaluate the  
 252 viscosity of the system, the tan ( $\delta$ ) was examined. Tan ( $\delta$ ) is a measure of the dampening in the  
 253 material and is the ratio of the loss ( $G''$ ) and the storage ( $G'$ ) modulus. A reduction of tan ( $\delta$ )  
 254 was observed with increased covalent crosslinking (e.g., greater PEG-DA concentration);  
 255 however, higher GH polymer concentrations resulted in a pronounced increase in tan ( $\delta$ ) (Fig.  
 256 3B). Moreover, tan ( $\delta$ ) was highly tunable through modulation of the GH to PEG-DA molar ratio  
 257 (Fig. 3C). Specifically, an increase in the relative GH concentration resulted in more viscous  
 258 behavior of the DN hydrogels as indicated by the increase of tan ( $\delta$ ). Taken together, the  
 259 findings demonstrate a system where the viscous and elastic properties can be modulated  
 260 independently. Although altering the elasticity of DN hydrogels with varying PEG-fibrinogen  
 261 amounts is possible, we chose a constant concentration of 8.5 mg/mL, which has been shown  
 262 to support homogenous hydrogel formation and cell compatibility<sup>26, 31</sup>. Importantly, DN  
 263 mechanical properties cover the range of viscoelasticity measured in a number of soft tissues,  
 264 including cardiac and skeletal muscle as well as lung tissue<sup>32</sup>. While other DN hydrogel systems  
 265 have demonstrated similar elastic properties<sup>18, 21-23</sup>, they often lack the tunable viscous aspects  
 266 that may be needed to mimic the viscoelastic properties of many soft tissues and ECM<sup>32, 33</sup>.



267  
 268 **Figure 3 Viscoelastic properties of DN hydrogels are tuned through the amount of**  
 269 **independent networks.**

270 Rheological measurements (1.0 Hz, 0.5% strain) of **A** storage modulus ( $G'$ ) and **B** tan ( $\delta$ ) for DN  
 271 hydrogels with PEG-fibrinogen (8.5 mg/mL) and varied GH (0, 3, 5%) and PEG-DA (1, 2, 3%)  
 272 concentrations (conc., n = 3 replicates per group, mean  $\pm$  SD, \*\*p  $\leq$  0.01 by one-way ANOVA with  
 273 Bonferroni *post hoc*). **C** Tan ( $\delta$ ) of DN hydrogels with various molar ratios of GH/PEG-DA (n = 3 replicates  
 274 per group, mean  $\pm$  SD). Colored symbols represent examples of DN hydrogels (PEG-fibrinogen (8.5  
 275 mg/mL) plus 2% PEG-DA) with varied GH concentrations.

276

277

278

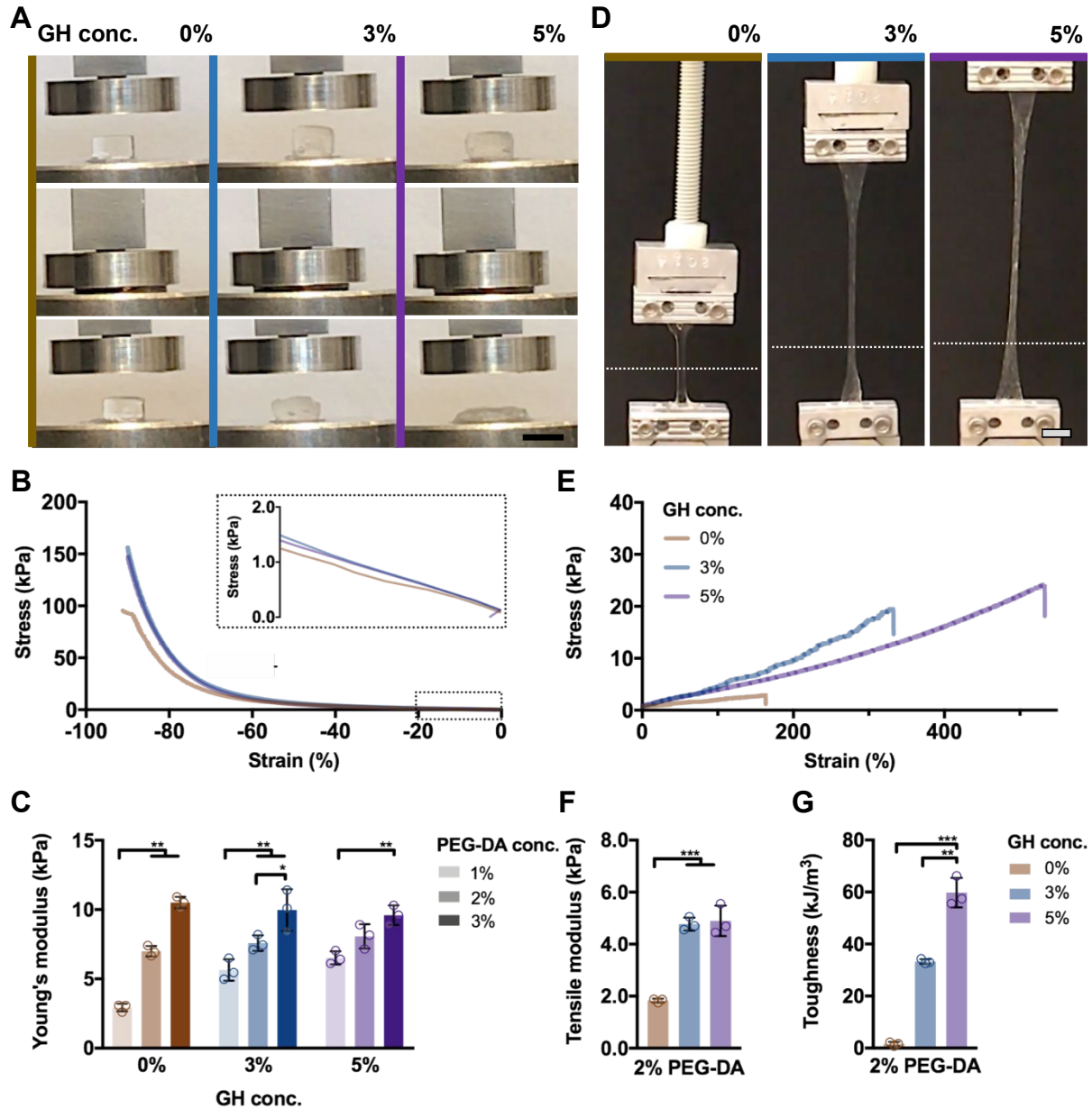
### 279 ***DNs exhibit high mechanical strength and toughness***

280 In addition to capturing the viscoelastic behavior of native ECM, high mechanical strength and  
281 toughness of hydrogels are often critical towards their applications in repair and augmentation of  
282 tissues. Since a high degree of tunability was observed with DN hydrogels with 2% PEG-DA,  
283 this covalent crosslink density was used in subsequent studies (unless otherwise noted) and the  
284 GH concentration was varied at 0%, 3%, and 5%. When tested in compression, PEG-fibrinogen  
285 hydrogels with only covalent crosslinking (0% GH) and DNs with 3% GH exhibited recovery  
286 following compression to 90% strain, whereas ductile and unrecoverable failure was observed  
287 for 5% DN hydrogels (Fig. 4A, Video S1), indicating that the ratio of covalent to supramolecular  
288 crosslinks is critical to DN hydrogel mechanics. Compressive stress-strain relationships  
289 demonstrated increased failure stresses for DN hydrogels over covalent-only hydrogels, but little  
290 changes in the moduli when compared with 0% GH (inset, Fig. 4B). Further, the dependence of  
291 the Young's modulus on PEG-DA concentration and only minimally on GH content was similar  
292 to observations by rheology, confirming the tunability of the system (Fig. 4C).

293 When subjected to tensile loading, elongation was observed for all hydrogels (Fig. 4D,  
294 Video S2). DN hydrogels exhibited approximately eight-fold and ten-fold increases in failure  
295 stresses at 3% and 5% GH concentrations, respectively, when compared to covalent-only  
296 hydrogels with similar improvements in failure strains (Fig. 4E, Fig. S4). Along with these  
297 changes in tensile properties, increased moduli were observed for DNs compared with 0% GH  
298 hydrogels (Fig. 4F). Despite similar tensile moduli for both 3% and 5% DNs, increasing GH  
299 concentrations further enhanced the toughness of DN hydrogels up to  $57.4 \pm 8.8 \text{ kJ m}^{-3}$  (Fig.  
300 4G).

301 Since the GH hydrogel assembly is reversible, DNs retained the ability to self-heal and  
302 undergo repeated mechanical loading. Cut hydrogel fragments exhibited rapid healing due to  
303 GH interactions, enabling resistance to separation (Video S3). Thus, supramolecular  
304 interactions endowed DNs with enhanced compressive and tensile strengths as well as the  
305 ability to withstand repeated loading, properties that may be very useful depending on their  
306 application.

307



308

309

**Figure 4 DN hydrogels exhibit high mechanical strength and toughness.**

310

**A-C** Compressive and **D-G** tensile testing of DN hydrogels (PEG-fibrinogen (8.5 mg/mL) plus 2% PEG-DA) without (0%) or with (3%, 5%) GH of different concentrations. **A** Images of DN hydrogel compressive testing (scale bars 5 mm) and corresponding **B** stress-strain profiles (0.5 N min<sup>-1</sup>) and **C** Young's moduli (n = 3 replicates per group, mean ± SD, \*\*p ≤ 0.01) for DN hydrogels. **D** Images of DN hydrogel tensile testing, where the starting position of the top grid is indicated (dotted line, scale bars 5 mm) and corresponding **E** stress-strain profiles (5 mm/sec<sup>-1</sup>), **F** tensile moduli, and **G** toughness for DN hydrogels (n = 3 replicates per group, mean ± SD, \*\*p ≤ 0.01, \*\*\*p ≤ 0.001).

317

318

319

320

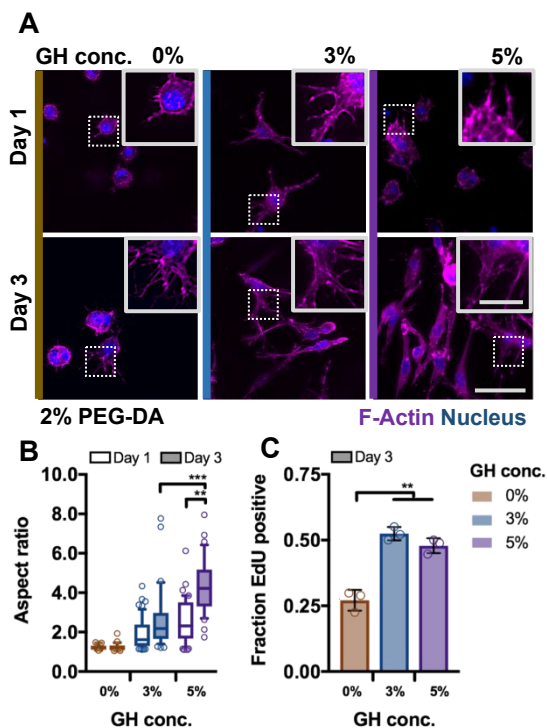
### 321 ***DNs enable control over cell behavior in 3D hydrogels***

322 In addition to providing mechanical support and resilience, cytocompatibility and matrix  
323 remodeling are critical towards functional tissue repair; however, these cellular processes are  
324 limited in many hydrogels, including with many DN systems. Using the hydrogel system  
325 developed, we investigated the influence of DN hydrogel properties - the same elasticity ( $G'$   $2.4$   
326  $\pm 0.26$  kPa) but altered viscosity ( $G''$   $0.00 - 1.34$  kPa, Fig. 5A) - on cell morphology and activity.  
327 Encapsulated MSCs exhibited high viability ( $>85\%$ ) in all conditions throughout three days in  
328 culture (Fig. S5). To examine cell morphologies in these hydrogels, cytoskeletal organization  
329 was visualized using F-Actin staining (Fig. 5A). After one day of culture in growth media,  
330 encapsulated MSCs exhibited generally rounded morphologies with some protrusions across all  
331 hydrogels. However, after three days, cell spreading was greatly enhanced in DN hydrogels  
332 ( $3\%$ ,  $5\%$ ) - cells in both conditions adopted spindle-like morphologies with thin and elongated  
333 protrusions.

334 When comparing temporal profiles of cell spreading with increasing GH concentrations,  
335 cell aspect ratios (a measure of spreading) increased as a function of viscosity and time (Fig.  
336 5B). No significant differences in aspect ratios were observed for cells in covalent only ( $0\%$  GH)  
337 hydrogels following three days of culture. Functional outcomes of cell spreading were also  
338 altered; MSC proliferation in DNs, as assayed by EdU incorporation (Fig. S6), was enhanced by  
339  $\sim 25\%$  of values in  $0\%$  GH hydrogels (Fig. 5C). It should be noted that the fibrinogen backbone  
340 of these hydrogels is susceptible to degradation by proteinases (Fig. S7). Although protrusions  
341 in  $0\%$  GH hydrogel matrices indicated that cells have started to proteolytically degrade their  
342 matrix environment within three days, remodeling of such dense polymer networks likely  
343 necessitates longer culture times<sup>25, 26</sup>.

344 Taken together, these findings suggest that cellular remodeling of DN hydrogels allows  
345 for cell spreading and proliferation when compared to the purely covalently crosslinked  
346 hydrogels. Moreover, cell behavior is regulated by cell-mediated rearrangement of the dynamic  
347 GH bonds, and emphasizes, consistent with previous reports<sup>9, 11</sup>, that cells respond to the  
348 increasing viscosity (i.e. higher GH concentration) of the hydrogel microenvironment. Notably,  
349 we found that network rearrangements occurred quickly (within three days) through cellular  
350 remodeling to influence cell spreading and proliferation. This link between hydrogel remodeling  
351 and cell response suggests that the rapid dynamics of GH bonds not only enable encapsulated  
352 MSCs to rearrange their microenvironment, but also influence cell activity and function.  
353 Although the molecular mechanisms remain to be elucidated, an increase in ligand density and  
354 integrin clustering has been found to be critical for activating signaling pathways that mediate

355 cell spreading in viscoelastic hydrogels<sup>9, 10, 34</sup>. Other dynamic systems (e.g., ionic<sup>9</sup>, dynamic  
 356 covalent bonds<sup>35</sup>) often require several days for cellular remodeling; thus, this DN hydrogel may  
 357 add a valuable strategy for capturing ECM dynamics at varying time scales<sup>36, 37</sup>. Beyond  
 358 studying cell behavior *in vitro*, the identified network structural parameters may be harnessed to  
 359 accommodate the dynamic needs during tissue healing and can be further engineered to  
 360 enhance endogenous repair (e.g., through release of growth factors<sup>38, 39</sup>, chemoattractants<sup>39</sup>,  
 361 cytokines<sup>40</sup>). Recent work demonstrating enhanced cell invasion and tissue formation through  
 362 introducing viscosity to implanted hydrogels illustrates this potential<sup>41</sup>.



363

### 364 **Figure 5 DN hydrogels are cytocompatible and enable control over cell spreading.**

365 **A** Representative images of F-Actin immunofluorescence of bovine MSCs cultured for one and three days  
 366 in DN hydrogels (PEG-fibrinogen (8.5 mg/mL) plus 2% PEG-DA) without (0%) or with (3% or 5%) GH of  
 367 different concentrations (scale bar 50  $\mu$ m, inset 20  $\mu$ m). Quantification of **B** cell aspect ratio ( $n \geq 50$  cells  
 368 per group, box plots show 25/50/75th percentiles, whiskers show 10/90th percentiles, \*\*  $p \leq 0.01$ , \*\*\* $p \leq$   
 369 0.001 by one-way ANOVA with Bonferroni *post hoc*) after one and three days of culture and **C** fraction of  
 370 cells after three days of culture with nuclei positively stained for 5-Ethynyl-2'-deoxyuridine (EdU,  $n = 3$   
 371 replicates per group, mean  $\pm$  SD, \*\*  $p \leq 0.01$  by one-way ANOVA with Bonferroni *post hoc*).

372

373

### 374 **Conclusions**

375 Supramolecular and covalent interactions were used to form DN hydrogels that are viscoelastic  
 376 to create dynamic matrices for cell encapsulation. Network entanglement resulted in the desired  
 377 hydrogel properties with enhanced mechanical strength and toughness when compared to

378 single-network hydrogels. Owing to rapid association of supramolecular bonds, internal self-  
379 healing of DN hydrogels resulted in recoverable primary networks, enabling repetitive loading.  
380 Furthermore, the viscoelastic properties were controlled independently through alterations of the  
381 concentration of either network. Using this tunability, an increase in network viscosity (e.g.  
382 through higher supramolecular polymer concentration) influenced cell behavior, enhancing cell  
383 spreading and proliferation. The ability of this system to not only enable cellular remodeling, but  
384 also recapitulate the mechanical resilience of many tissues may provide new avenues towards  
385 functional tissue repair.

386

### 387 **Acknowledgements**

388 This work was financially supported by the National Science Foundation (JAB: DMR Award  
389 1610525, JHG: Graduate Research Fellowship), the Swiss National Science Foundation (CL),  
390 the USA-Israel Binational Science Foundation (DS, AA, OK, HSY: Award 2015697), and the  
391 Israel Science Foundation (DS, OK: Award 1245/14). The authors thank the Penn Center for  
392 Musculoskeletal Disorders for tensile testing.

393

394

395

396

### References

- 397 1. D. Seliktar, *Science*, 2012, **336**, 1124-1128.
- 398 2. M. Guvendiren and J. A. Burdick, *Current Opinion in Biotechnology*, 2013, **24**, 841-846.
- 399 3. S. R. Caliari and J. A. Burdick, *Nat Methods*, 2016, **13**, 405-414.
- 400 4. S. Khetan, M. Guvendiren, W. R. Legant, D. M. Cohen, C. S. Chen and J. A. Burdick,  
401 *Nat Mater*, 2013, **12**, 458-465.
- 402 5. K. M. Schultz, K. A. Kyburz and K. S. Anseth, *Proc Natl Acad Sci U S A*, 2015, **112**,  
403 E3757-3764.
- 404 6. S. B. Anderson, C. C. Lin, D. V. Kuntzler and K. S. Anseth, *Biomaterials*, 2011, **32**,  
405 3564-3574.
- 406 7. S. J. Bryant and K. S. Anseth, *J Biomed Mater Res A*, 2003, **64**, 70-79.
- 407 8. S. Sahoo, C. Chung, S. Khetan and J. A. Burdick, *Biomacromolecules*, 2008, **9**, 1088-  
408 1092.
- 409 9. O. Chaudhuri, L. Gu, D. Klumpers, M. Darnell, S. A. Bencherif, J. C. Weaver, N.  
410 Huebsch, H. P. Lee, E. Lippens, G. N. Duda and D. J. Mooney, *Nat Mater*, 2016, **15**,  
411 326-334.
- 412 10. J. Lou, R. Stowers, S. Nam, Y. Xia and O. Chaudhuri, *Biomaterials*, 2018, **154**, 213-222.
- 413 11. A. R. Cameron, J. E. Frith and J. J. Cooper-White, *Biomaterials*, 2011, **32**, 5979-5993.
- 414 12. H. Shih and C.-C. Lin, *Journal of Materials Chemistry B*, 2016, **4**, 4969-4974.
- 415 13. A. M. Rosales, S. L. Vega, F. W. DelRio, J. A. Burdick and K. S. Anseth, *Angewandte*  
416 *Chemie International Edition*, 2017, **56**, 12132-12136.
- 417 14. J. P. Gong, Y. Katsuyama, T. Kurokawa and Y. Osada, *Advanced Materials*, 2003, **15**,  
418 1155-1158.
- 419 15. M. A. Haque, T. Kurokawa and J. P. Gong, *Polymer*, 2012, **53**, 1805-1822.
- 420 16. X. Zhao, *Soft Matter*, 2014, **10**, 672-687.



- 421 17. O. Jeon, J.-Y. Shin, R. Marks, M. Hopkins, T.-H. Kim, H.-H. Park and E. Alsberg,  
422 *Chemistry of Materials*, 2017, **29**, 8425-8432.
- 423 18. Z. Liang, C. Liu, L. Li, P. Xu, G. Luo, M. Ding and Q. Liang, *Sci Rep*, 2016, **6**, 33462.
- 424 19. J.-Y. Sun, X. Zhao, W. R. K. Illeperuma, O. Chaudhuri, K. H. Oh, D. J. Mooney, J. J.  
425 Vlassak and Z. Suo, *Nature*, 2012, **489**, 133.
- 426 20. M. Guo, L. M. Pitet, H. M. Wyss, M. Vos, P. Y. W. Dankers and E. W. Meijer, *Journal of*  
427 *the American Chemical Society*, 2014, **136**, 6969-6977.
- 428 21. C. B. Rodell, N. N. Dusaj, C. B. Highley and J. A. Burdick, *Adv Mater*, 2016, **28**, 8419-  
429 8424.
- 430 22. C. Li, M. J. Rowland, Y. Shao, T. Cao, C. Chen, H. Jia, X. Zhou, Z. Yang, O. A.  
431 Scherman and D. Liu, *Adv Mater*, 2015, **27**, 3298-3304.
- 432 23. Y. Yan, M. Li, D. Yang, Q. Wang, F. Liang, X. Qu, D. Qiu and Z. Yang,  
433 *Biomacromolecules*, 2017, **18**, 2128-2138.
- 434 24. L. Almany and D. Seliktar, *Biomaterials*, 2005, **26**, 2467-2477.
- 435 25. D. Dikovsky, H. Bianco-Peled and D. Seliktar, *Biophysical Journal*, 2008, **94**, 2914-2925.
- 436 26. D. Dikovsky, H. Bianco-Peled and D. Seliktar, *Biomaterials*, 2006, **27**, 1496-1506.
- 437 27. C. Loebel, C. B. Rodell, M. H. Chen and J. A. Burdick, *Nat Protoc*, 2017, **12**, 1521-1541.
- 438 28. C. B. Rodell, A. L. Kaminski and J. A. Burdick, *Biomacromolecules*, 2013, **14**, 4125-  
439 4134.
- 440 29. C. Loebel, S. E. Szczesny, B. D. Cosgrove, M. Alini, M. Zenobi-Wong, R. L. Mauck and  
441 D. Eglin, *Biomacromolecules*, 2017, **18**, 855-864.
- 442 30. A. M. S. Costa and J. F. Mano, *European Polymer Journal*, 2015, **72**, 344-364.
- 443 31. I. Mironi-Harpaz, D. Y. Wang, S. Venkatraman and D. Seliktar, *Acta Biomaterialia*, 2012,  
444 **8**, 1838-1848.
- 445 32. I. Levental, P. C. Georges and P. A. Janmey, *Soft Matter*, 2007, **3**, 299-306.
- 446 33. O. Chaudhuri, *Biomater Sci*, 2017, **5**, 1480-1490.
- 447 34. G. Maheshwari, G. Brown, D. A. Lauffenburger, A. Wells and L. G. Griffith, *Journal of*  
448 *Cell Science*, 2000, **113**, 1677-1686.
- 449 35. D. D. McKinnon, D. W. Domaille, J. N. Cha and K. S. Anseth, *Adv Mater*, 2014, **26**, 865-  
450 872.
- 451 36. H. Wang and S. C. Heilshorn, *Advanced Materials*, 2015, **27**, 3717-3736.
- 452 37. L. Li, J. Eyckmans and C. S. Chen, *Nature Materials*, 2017, **16**, 1164.
- 453 38. A. Shekaran, J. R. Garcia, A. Y. Clark, T. E. Kavanaugh, A. S. Lin, R. E. Guldberg and  
454 A. J. Garcia, *Biomaterials*, 2014, **35**, 5453-5461.
- 455 39. C. H. Lee, F. Y. Lee, S. Tarafder, K. Kao, Y. Jun, G. Yang and J. J. Mao, *J Clin Invest*,  
456 2015, **125**, 2690-2701.
- 457 40. K. L. Spiller, S. Nassiri, C. E. Witherel, R. R. Anfang, J. Ng, K. R. Nakazawa, T. Yu and  
458 G. Vunjak-Novakovic, *Biomaterials*, 2015, **37**, 194-207.
- 459 41. M. Darnell, S. Young, L. Gu, N. Shah, E. Lippens, J. Weaver, G. Duda and D. Mooney,  
460 *Adv Healthc Mater*, 2017, **6**.
- 461